

# SUBSTRATE INTEGRATED WAVEGUIDE FILTERS BASED ON EVEN- AND ODD-MODE PREDISTORTION TECHNIQUE

Z. Zakaria<sup>1</sup>, Ian C. Hunter<sup>2</sup>

<sup>1</sup>Faculty of Electronic and Computer Engineering,  
Universiti Teknikal Malaysia Melaka UTeM  
Hang Tuah Jaya 76100, Melaka, Malaysia,

<sup>2</sup>School Electronic & Electrical Engineering,  
University of Leeds LS2 9JT Leeds, United Kingdom

Email: zahriladha@utem.edu.my

## Abstract

*Novel techniques for the design of predistorted Substrate Integrated Waveguide (SIW) bandpass and bandstop filter are presented. The techniques allow for the realization of lossy filters with ideal lossless transmission and reflection response, offset by a constant amount. Two prototype third-degree Chebyshev bandpass and Inverse Chebyshev bandstop filters are proposed and designed. The two SIW filters having the same center frequency of 6.5 GHz and bandwidth of 125 MHz are implemented on RT/Duroid 4350 substrate with thickness of 0.508 mm. Experimental results show excellent agreement with simulated performance. These new class of filters would be useful in microwave systems where the increased insertion loss can be tolerated, such as in a satellite IMUX.*

**Keywords:** Bandpass filters, bandstop filters, lossy filters, Substrate Integrated Waveguide.

## I. INTRODUCTION

MICROWAVE filters play an important role in various aspects in communication systems. However, due to demand in emerging applications such as in wireless communication, filter designers have to find solutions to fulfill more important requirements such as higher performance, smaller size, lighter weight, and lower cost. A multiplexer of a satellite payload is one of the applications where there can be as many as 100 channels [1]. These multiplexers make up a large part of the communication payload, and therefore reducing the size and weight of them becomes very important.

It is well known that the performance of highly selective filters depends strongly on having high resonator unloaded- $Q$  ( $Q_u$ ) factor. However, this will result in significant physical volume or expensive technologies. It is therefore, preferable to design a filter in such a way that losses are taken into account and compensated for, in the process of minimizing the required  $Q_u$  factor, and consequently decreasing the size and expense of the filter.

Let us consider an approximate formula for Chebyshev filters to determine midband insertion loss is [2]:

$$LA_o = 8.686[N - 1.5] \frac{f_o}{\Delta f Q_u} \quad (1)$$

As an example, consider an eight-pole filter centered at 10 GHz with 10 MHz bandwidth. For a passband insertion loss of 1 dB, the approximate  $Q_u$  factor is 56,500. In contrast, for 6 dB loss, the approximate  $Q_u$  factor is 9,410. The latter gives just around six times reduction in  $Q_u$  factor. It has been proven that a specification with 6 dB loss is applicable for receive filters particularly input multiplexer (IMUX) in satellite communications [3]. This is because in the absence of large interfering signals it is possible to tolerate significant filter passband loss of 6 dB by preceding the filter by a low-noise amplifier.

The challenge is now to design such a selective filter with low- $Q_u$  resonators

without degrading the performance for the desired applications. This has led to the research and development of filter synthesis for loss compensation techniques. The first example of this work is known as classical predistortion [4]. However, it was proved in [3] that predistorted bandpass filters suffer from poor return loss, and thus require the use of isolators in practice. This problem could be avoided with the nonuniform- $Q_u$  factor design technique given in [5], however, this technique becomes more complex for higher orders, and computer optimization is required. The other technique is predistorted reflection-mode filters, but this technique requires the use of circulators [6]. Further improvement was made in [7] to avoid the use of the circulator by introducing a hybrid  $90^\circ$  coupler. Based on this technique, the even- and odd-mode reflection coefficients of a lossless filter are individually predistorted, and attached to a hybrid  $90^\circ$  coupler to reconstruct the full response. However, the use of hybrid  $90^\circ$  coupler still adds the complexity and size to the circuit.

In this paper, a symmetrical filter network based upon predistorted even- and odd-mode subnetworks analysis to design SIW filters is presented. The advantages of this technique that has been shown for the first time in [8] are the realizations of lossy filters response that equivalent to an ideal lossless filters, that are offset by a constant amount and do not require non-reciprocal devices.

This paper is organized as follows. In section II, the theory of even- and odd-mode predistortion technique is described, followed by overview of Substrate Integrated Waveguide (SIW). Section III provides the designs and realizations of SIW bandpass and bandstop filters along with experimental results and, finally, Section IV concludes this study.

## II. THEORY

### A. Even- and Odd-Mode Predistortion

The technique of even- and odd-mode has been well explained in [8],[9] and summarized as follows:

- i. Derive the even- and odd-mode reflection coefficients  $S_e(p)$  and  $S_o(p)$  from  $S_{11}(p)$  and  $S_{12}(p)$  of a symmetrical lossless filter.

$$S_e(p) = K(S_{11}(p) + S_{12}(p)) \quad (2)$$

$$S_o(p) = K(S_{11}(p) - S_{12}(p)) \quad (3)$$

$K$  is a constant with value less than 1

- ii. Apply predistortion to  $S_e(p)$  and  $S_o(p)$ .

$$S_e(p) \rightarrow K(p - \alpha_e) \quad (4)$$

$$S_o(p) \rightarrow K(p - \alpha_o) \quad (5)$$

- iii. Determine the dissipation factors  $\alpha_e$  and  $\alpha_o$  such that the magnitudes of the respective reflection coefficient peaks are unity at  $\omega_p$  with the following conditions:

$$|S_e(j\omega - \alpha_e)|_{\omega=\omega_0}^2 = 1 \quad (6)$$

$$\frac{d}{d\omega} |S_e(j\omega - \alpha_e)|_{\omega=\omega_0}^2 = 0 \quad (7)$$

$$|S_o(j\omega - \alpha_o)|_{\omega=\omega_0}^2 = 1 \quad (8)$$

$$\frac{d}{d\omega} |S_o(j\omega - \alpha_o)|_{\omega=\omega_0}^2 = 0 \quad (9)$$

- iv. Synthesize using cascade synthesis as described in [6],[7]. A first-order Singlet section is used to extract a single transmission zero whilst a second-order Brune section is used to extract two transmission zeros. This produces a cascade of Singlet or Brune sections terminated in a lossy resonator or a resistor.

- v. Develop a symmetrical network from the synthesized even- and odd-mode predistorted subnetworks.

Fig. 1 and 2 show the resulting third-order Butterworth lowpass prototype and its response based on even- and odd-mode predistortion technique. The shaded circles represent 1 Farad capacitors with a given loss factor. Admittance inverters are represented by connecting lines and un-shaded circles represent nodes. The lowpass prototype contains two high- $Q_u$  resonators ( $Q_u = 6.41$ ) and one low- $Q_u$  resonator ( $Q_u = 3$ ).

A third-order highpass prototype can also be designed using a similar method by interchanging the transmission and reflection responses,  $S_{11}(p)$  and  $S_{12}(p)$ . As the stand-alone conductances of the subnetworks are the inverse of one another, when the subnetworks are combined to form a symmetrical network, the conductances from a matched attenuator gives an attenuation equal to the multiplicative constant  $K$ , used in equations (3) and (4). For example, when  $K = 0.5$ , 6 dB of attenuation is provided. The highpass prototype and its response are shown in Fig. 3 and 4.

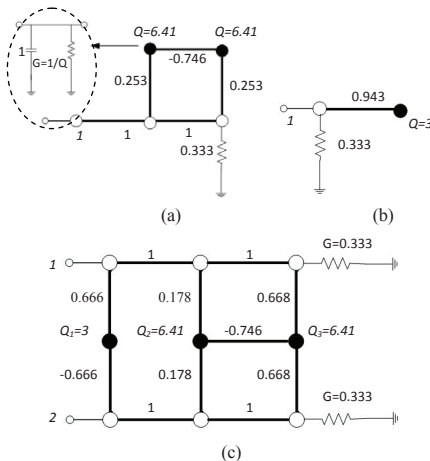


Fig. 1. 3<sup>rd</sup>-order Butterworth lowpass prototype. (a) Even-mode subnetwork. (b) Odd-mode subnetwork. (c) Cascade configuration of even- and odd-mode subnetworks and forming a mirror image [8].

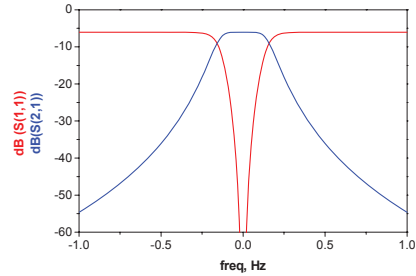


Fig. 2. Ideal third-order Butterworth lowpass response offset by 6 dB.

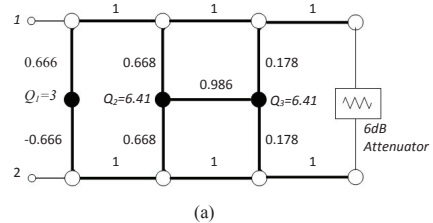


Fig. 3. Simplified 3<sup>rd</sup>-order Butterworth highpass prototype [8].

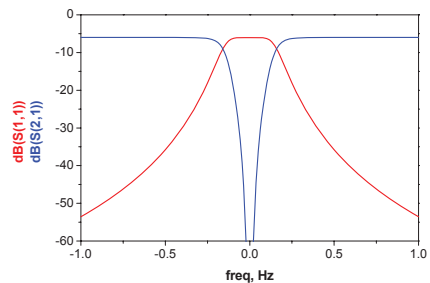


Fig. 4. Ideal 3<sup>rd</sup>-order Butterworth highpass response.

## B. Substrate Integrated Waveguide (SIW)

Substrate Integrated Waveguide (SIW) is defined as a waveguide synthesized within a dielectric substrate and the propagating waves are delimited by arrays of via holes as illustrated in Fig. 5. A periodic via hole structure is constructed to realize the bilateral edge walls. Fig. 5(c) shows a SIW with an array of via holes while the substrate height,  $b$  and the distance between the parallel arrays of via holes are shown in Fig. 5(b). It is well known that the propagation constant of the  $TE_{10}$  mode is

only related to the width  $a$ ; therefore, the height or thickness  $b$ , of the waveguide can be reduced with minimal influence on the  $TE_{10}$  propagation, thus, allowing its integration into a thin substrate. Fig. 6 explains the effect of arrays of via holes which acting as a boundary to prevent the escape of electric fields, thus, an artificial wall is provided with properties similar to a waveguide.

The SIW has been studied by many researchers since its introduction in 2001 by Ke Wu [10]. The concept of SIW filters have been discussed in details in [11], while the optimization of the cavity shape has also been analyzed in [12]. The procedure to develop a SIW cavity resonator is summarized as follows:

- i. If the mode of propagation in the waveguide is a  $TE_{10}$  along  $z$ , then the  $E$  field must be zero at  $z = 0$  and  $z = l$ . Then  $l$  must be a half of a guided wavelength. Therefore;

$$l = \frac{\lambda_g}{2} = \frac{\lambda_0}{2 \left[ 1 - \left( \frac{a}{2l} \right)^2 \right]^{\frac{1}{2}}} = \frac{\lambda_0}{2 \left[ 1 - \left( \frac{\lambda_0}{2l} \right)^2 \right]^{\frac{1}{2}}} \quad (11)$$

The resonant frequency can be determined using;

$$f_0 = \frac{c}{\lambda_0} = \frac{c(a^2 + l^2)^{\frac{1}{2}}}{2al} \quad (12)$$

Thus, the width  $a$ , of the waveguide can be determined using equation (11).

- ii. The transformation to rectangular SIW is implemented by simply dividing the length  $l$ , and width  $a$ , with  $\sqrt{\epsilon_r}$ .
- iii. The effective dimension of SIW cavity can be determined by the corresponding frequency form [13];

$$f_r = \frac{c}{2\pi \sqrt{\mu_r \epsilon_r}} \sqrt{\left( \frac{\pi^2}{a_{eff}} \right)^2 + \left( \frac{\pi}{l_{eff}} \right)^2} \quad (13)$$

where  $a_{eff}$  and  $l_{eff}$  are the effective width and length of the resonant SIW cavity given by;

$$l_{eff} = l_r - \frac{d^2}{0.95p} \quad (14)$$

and

$$a_{eff} = a_r - \frac{d^2}{0.95p} \quad (15)$$

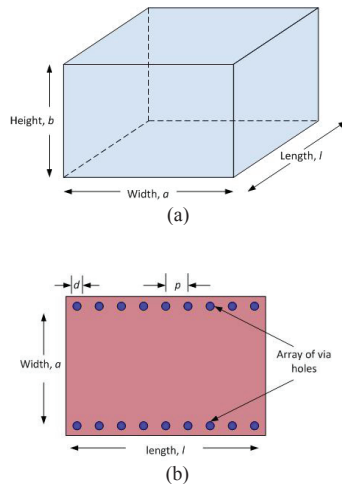
Here,  $l_r$  and  $a_r$  are the real width and length of the SIW cavity,  $d$  and  $p$  are the diameter and the distance between adjacent vias respectively. The constant  $c$  is the speed of light in free space where  $\mu_r$  and  $\epsilon_r$  are the relative permeability and the relative permittivity of the substrate, respectively.

- iv. From a practical point of view, via hole diameter  $d$ , and its pitch  $p$ , can be calculated using [14], [15];

$$d > 0.2\lambda_0 \quad (16)$$

and

$$\frac{d}{p} \leq 0.5 \quad (17)$$



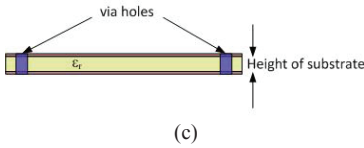


Fig. 5. On-substrate synthesis techniques: a) a rectangular waveguide resonator; b) a SIW with metallised via holes; c) front view via holes inside the SIW.

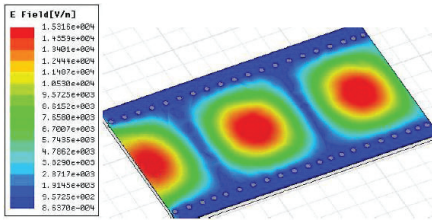


Fig. 6. Electromagnetic simulation showing magnitude of E field [16].

### III. PRACTICAL FILTERS DESIGN

In this section, a systematic filter development using the lowpass and highpass prototype as a starting point will be demonstrated. The Chebyshev response is used in this example because it is generally well-known and widely used. It is also own a relatively high selectivity characteristic compared to the Butterworth response. Therefore, using the method discussed in Section III (A), a 3<sup>rd</sup>-order Chebyshev lowpass prototype network can be established. The simplified network and its response are shown in Fig.7. The lowpass prototype contains two high-  $Q_u$  factor resonators ( $Q_u = 5.39$ ) and one low- $Q_u$  factor resonator ( $Q_u = 2.558$ ). This lowpass prototype is used to develop a bandpass filter.

Similarly for the highpass prototype, it can be constructed by interchanging the transmission and reflection responses,  $S_{11}(p)$  and  $S_{12}(p)$ . The element values are obtained in the same instance as for the lowpass prototype except the conductances from a matched attenuator now give an attenuation equal to the multiplicative constant  $K$  as shown in Fig. 8. The symmetrical network also contains

two high-  $Q_u$  factor resonators ( $Q_u = 5.39$ ) and one low-  $Q_u$  factor resonator ( $Q_u = 2.558$ ). This highpass prototype is used to develop a bandstop filter to exhibit an inverse Chebyshev response.

#### A. Bandpass Filter

For realization purposes, the lowpass prototype is transformed to a bandpass filter using standard transformation. The theory behind the transformation is well explained in [17]. The focus here is on the resonators and their lowpass to bandpass transformations, as shown in Fig. 9.

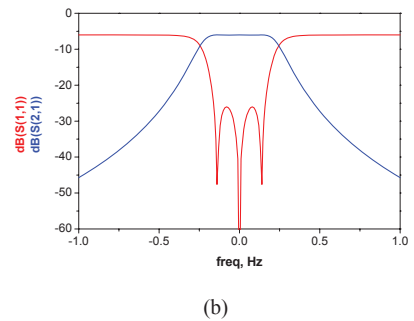
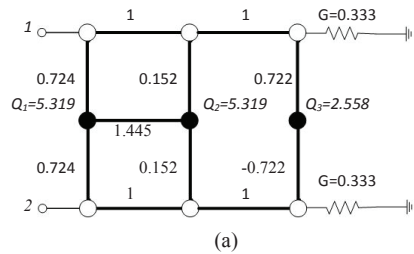
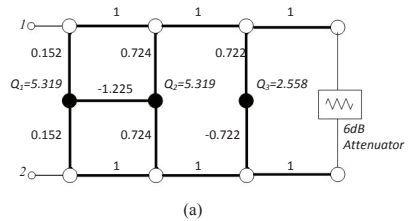
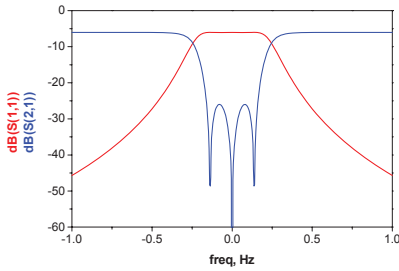


Fig. 7. Ideal 3<sup>rd</sup>-order Chebyshev lowpass prototype (a) simplified circuit (b) response with 6 dB offset.





(b)

Fig. 8. Ideal 3<sup>rd</sup>-order Chebyshev highpass prototype (a) simplified circuit (b) response with 6 dB offset.

Design example: Center frequency,  $f_0$  at 6.5 GHz with 125 MHz fractional bandwidth. The following equations for the bandpass transformation of a capacitor of the lowpass prototype (Fig. 9) are applied to obtain element values for element capacitors and inductors [17];

Design example: Center frequency,  $f_0$  at 6.5 GHz with 125 MHz fractional bandwidth. The following equations for the bandpass transformation of a capacitor of the lowpass prototype (Fig. 9) are applied to obtain element values for element capacitors and inductors [17];

$$C'_r = \frac{\alpha' C_r}{\omega_0} \tag{18}$$

$$L'_r = \frac{1}{\alpha' C_r \omega_0} \tag{19}$$

where  $\alpha'$  is the bandwidth scaling factor,

$$\alpha' = \frac{\omega_0}{\omega_2 - \omega_1} \tag{20}$$

After scaling to 50  $\Omega$  the new element values for bandpass resonators are  $2.5465 \times 10^{-11}$  F and  $2.3544 \times 10^{-11}$  H. The resistive element for the first and second resonator is 265.95  $\Omega$  and 127.90  $\Omega$  for the third resonator. The unloaded-  $Q_u$  factor for this circuit is calculated using:

$$Q_u = \frac{f_0}{\Delta f} \frac{1}{\alpha} \tag{21}$$

where  $\alpha$  is loss factor from the lowpass prototype.

The bandpass filter now contains two high-  $Q_u$  resonators ( $Q_u = 276.59$ ) and one low-  $Q_u$  resonator ( $Q_u = 133.02$ ). Thus, the average  $Q_u$  factor is 238.26 and the filter is suitable to be realized in Substrate Integrated Waveguide (SIW) resonators [16],[18],[19],[20]. The response of the 3<sup>rd</sup>-order Chebyshev bandpass filter is shown in Fig. 10 with passband insertion loss and return loss values of 6 dB and 26 dB respectively

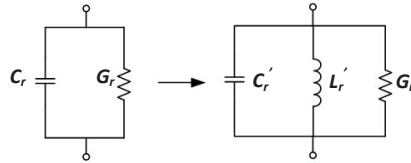


Fig. 9. Bandpass transformation of a capacitor with dissipative.

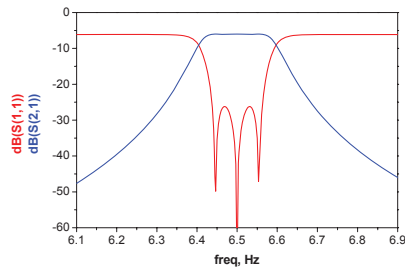


Fig. 10. Ideal response of 3<sup>rd</sup>-order bandpass filter with Chebyshev response.

Certain modifications on the circuit are needed for practical physical realization. For instance, the resistive loads on the ends of both main-lines are scaled to 50  $\Omega$ , therefore, additional transmission lines are introduced in order to allow 50  $\Omega$  terminations for each main-line. Furthermore, the admittance inverter main-lines are replaced with  $3\lambda/4$  microstrip lines in order to accommodate the separation between the SIW resonator cavities. Admittances, or impedances, can be scaled to produce realizable values for ease of manufacturing process capability. The modified circuit for practical purposes is shown in Fig. 11.

The procedures discussed in Section II (B) are used to realize SIW resonators. The dimensions of rectangular waveguide

for  $TE_{10}$  mode operation with cut-off frequency of 4.301 GHz can be found using equations (11) and (12). These dimensions can be verified with the standard rectangular waveguide data [21]. The transformation to rectangular SIW is done simply by dividing the length,  $l$ , and width,  $a$ , of the rectangular waveguide with  $\sqrt{\epsilon_r}$ . The equivalent dimensions of the SIW cavity together via holes can be determined by applying equations (13) to (15) to obtain the effective width,  $a_{eff}$ , and length,  $l_{eff}$ , of the resonant SIW cavity. The rules described in equations (16) and (17) are applied to determine the size of via holes and the distance between them. In this case, a diameter and distance of 0.8 mm and 1.6 mm is calculated, respectively. All these dimensions can be further tuned and optimized during the simulation in order to obtain the desired responses.

The transition method from a rectangular SIW cavity to microstrip line is realized through coupling slot. Parameters such as penetration of slot  $S_1$  and slot gap  $S_g$  (as shown in Fig. 12(a)) are crucial and need to be carefully designed and optimized during the simulation. In this case, the responses for each SIW resonator must be reasonably matched with the ideal responses exhibited from the ideal circuits. The coupling between first and second resonators is realized based on iris. They are connected through microstrip line in order to have a  $3\lambda/4$  separation between the SIW resonator cavities. The design of inter-resonators coupling can be modeled during the simulation.

All the three SIW resonators can be merged with microstrip main-line to form an advanced bandpass filter; a combination of SIW and planar technology as shown in Fig. 13. The overall tuning and optimization process is implemented intensively, thus, a high performance with sufficiently large memory of computer would be required for these simulations. The physical coupling slot parameters are listed in Table I.

To verify the theory and simulation, the design is manufactured using a standard PCB process. The device is constructed using a 0.508 mm thick, Roger RO4350, dielectric substrate with permittivity constant  $\epsilon_r = 3.48$ . The copper thickness of copper is  $35\mu\text{m}$  and loss tangent is 0.0037.

The manufactured novel bandpass filter, with overall length and width dimension of 81.94 mm x 61.40 mm, is shown in Fig. 14. The comparison between measured and simulated responses is shown in Fig. 15. The measured results show the insertion loss ( $S_{21}$ ) is about -7.09 dB and return loss ( $S_{11}$ ) better than -19 dB are obtained in the passband. There is a frequency shift of 68 MHz from the desired center frequency. This is due to the variation of permittivity in the substrate and also manufacturing tolerance. The small amounts of losses in the passband are due to the losses of transition from microstrip to SIW, copper loss through conductivity, radiation loss through the surface of the SIW cavity, leakage through via holes and their pitches and losses through SMA connectors.

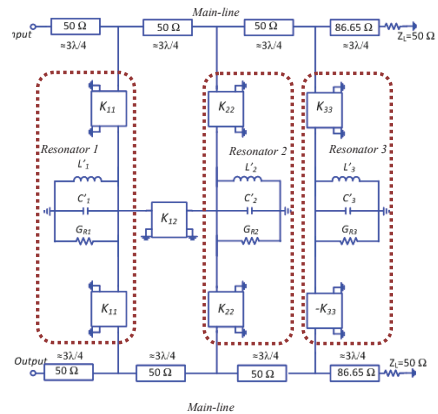


Fig. 11. Alternative circuit of bandpass filter.

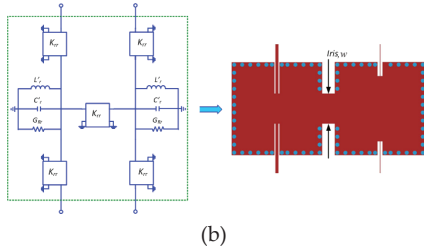
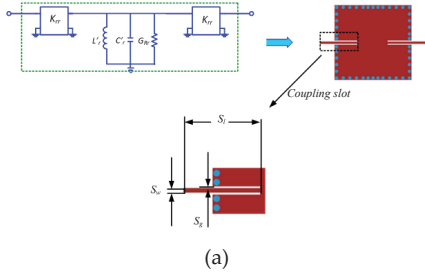


Fig. 12. (a) SIW cavity resonator with coupling slot. (b) Coupling between resonator 1 and 2.

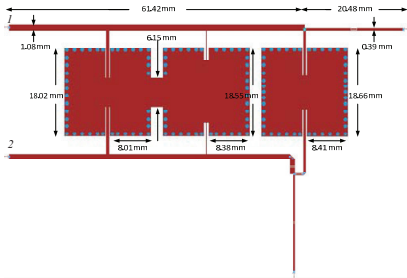


Fig. 13. Layout of SIW bandpass filter.

Table I. Coupling Slot Parameters

Resonator	$S_j$	$S_g$	$S_w$
$r=1$	9.68mm	0.1984mm	0.5958mm
$r=2$	6.34mm	0.4308mm	0.1284mm
$r=3$	9.34mm	0.215mm	0.5885mm

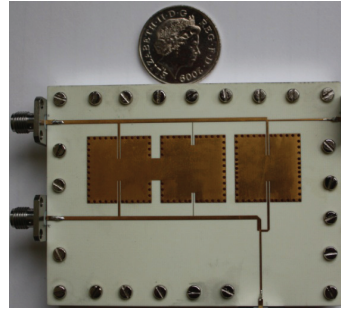


Fig. 14. Photograph of SIW bandpass filter.

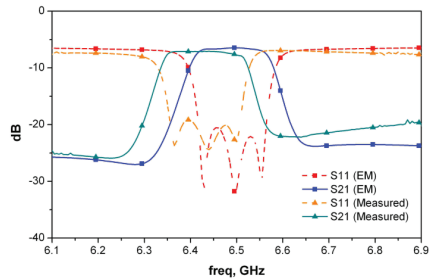


Fig. 15. SIW bandpass filter simulated and measured response.

### B. Bandstop Filter

The general steps to produce SIW bandstop filter is similar to the previous bandpass filter. It started from a highpass prototype (Fig. 8) followed by transformation to a bandstop filter using equations (18)-(20). Since a third-order Chebyshev highpass prototype is first defined, thus, the transformation will produce a bandstop filter with an inverse Chebyshev response.

A design example has the same center frequency and bandwidth as the previous example, i.e. 6.5 GHz and 125 MHz respectively. Thus it has identical unloaded-  $Q_u$  factor as bandpass filter, with average  $Q_u$  factor of 238.26 and, therefore, the filter is suitable to be realized in Substrate Integrated Waveguide (SIW). The inverse Chebyshev bandstop response is shown in Fig. 16. After the circuit is scaled to 50  $\Omega$  the new element values for bandstop resonators can be found, i.e.  $2.5465 \times 10^{-11}$  F and  $2.3544 \times 10^{-11}$  H. The resistive element for the first and



second resonator is  $265.95 \Omega$  and  $127.90 \Omega$  for the third resonator.

The bandstop filter can now be realized in SIW by applying the same method as for the SIW bandpass filter. The only difference here is negative coupling is applied between resonator 1 and 2; in which Potelon, *et.al* [22] have recently investigated a technique called grounded coplanar line can be used to produce negative coupling. The appropriate negative coupling can be achieved during the simulation by tuning the iris width,  $Cgl_w$ , slot width,  $Cgl_g$ , and its grounded coplanar line length,  $Cgl_l$ , as shown in Fig. 17. The bandstop filter is terminated with 6dB attenuator realized using chip attenuator.

The bandstop filter is modeled, simulated and optimized using ADS-Momentum. The model is shown in Fig. 18. The physical coupling slot and negative coupling parameters are listed in Table II. The model is then manufactured by using standard PCB process with the device constructed from Roger RO4350 on a 0.508 mm thick dielectric substrate with permittivity constant  $\epsilon_r = 3.48$ . Again, the copper thickness is  $35\mu\text{m}$  and loss tangent is 0.0037.

The manufactured novel bandstop filter, with final length and width dimensions of 93.10 mm x 58.51 mm, is shown in Fig. 18. The comparison between measured and simulated responses is shown in Fig. 19. The measured results show the  $S_{21}$  at passband is -7.23 dB while  $S_{21}$  with better than -21 dB is achieved in the stopband. There is a slight 65 MHz shift in frequency from the desired center frequency. This is due to the variation of permittivity in the substrate and also manufacturing tolerance. The small amounts of losses in the experimental results are due to the same factors as those in bandpass filter.

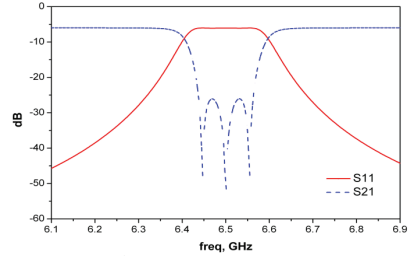


Fig. 16. Ideal 3<sup>rd</sup>-order bandstop filter with inverse-Chebyshev response.

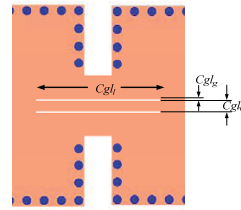


Fig. 17. Coupling between resonator 1 and 2.

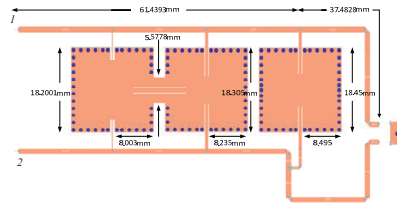


Fig. 18. Layout of SIW bandstop filter.

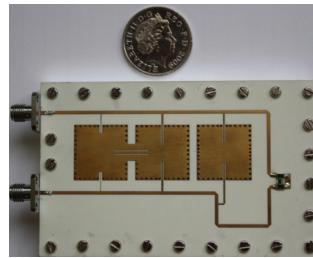


Fig. 19. Photograph of SIW bandstop filter.

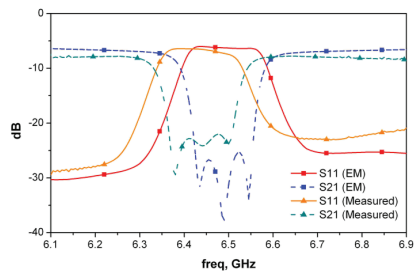


Fig. 20. SIW bandstop filter simulated and measured response.

IV. CONCLUSION

This study has demonstrated two novel designs of SIW lossy filter. This new class of microwave filters would be useful in any receiver systems whenever the increase of losses can be tolerated, and also when the reduction of size and weight are primary concerns, such as in the case of input multiplexers of the satellite transponder, wireless ground base stations, repeaters, etc. Since the technique of lossy filters presented in this study is still in its early stage of development, a lower degree filter has therefore been chosen in order to prove the concept, and also as a means of overcoming the physical realisation issues. The resulting lossy SIW filters exhibit ideal lossless responses with an offset of approximately 6 dB.

Table II. Coupling Slot Parameters

Resonator	$S_l$	$S_g$	$S_w$
$r=1$	6.288mm	0.44mm	0.1284mm
$r=2$	9.856mm	0.1999mm	0.5958mm
$r=3$	9.284mm	0.2267mm	0.5801mm
NEGATIVE COUPLING PARAMETERS			
$Cgl_l$	$Cgl_g$	$Sgl_w$	
11.5493mm	0.2008mm	1.008mm	

ACKNOWLEDGMENT

Z. Zakaria would like to thank the Government of Malaysia and UTeM for sponsoring this study.

REFERENCES

[1] M. Kunes, "Microwave multiplexers for space applications," *Electronics & Communication Engineering Journal*, vol. 10, pp. 29-35, 1998.

[2] I. Hunter, R. Ranson, A. Guyette, and A. Abunjaileh, "Microwave filter design from a systems perspective," *Microwave Magazine, IEEE*, vol. 8, pp. 71-77, 2007.

[3] I. Hunter, A. Guyette, and R. D. Pollard, "Passive microwave receive filter networks using low-Q resonators," *Microwave Magazine, IEEE*, vol. 6, pp. 46-53, 2005.

[4] M. Dshal, "Design of Dissipative Band-Pass Filters Producing Desired Exact Amplitude-Frequency Characteristics," *Proceedings of the IRE*, vol. 37, pp. 1050-1069, 1949.

[5] A. C. Guyette, I. C. Hunter, and R. D. Pollard, "The Design of Microwave Bandpass Filters Using Resonators With Nonuniform " Q", *Microwave Theory and Techniques, IEEE Transactions on*, vol. 54, pp. 3914-3922, 2006.

[6] W. M. Fathelbab, I. C. Hunter, and J. D. Rhodes, "Synthesis of lossy reflection-mode prototype networks with symmetrical and asymmetrical characteristics," *Microwaves, Antennas and Propagation, IEE Proceedings*, vol. 146, pp. 97-104, 1999.

[7] W. M. Fathelbab, I. C. Hunter, and J. D. Rhodes, "Synthesis of predistorted reflection-mode hybrid prototype networks with symmetrical and asymmetrical characteristics," *International Journal of Circuit Theory and Applications*, vol. 29, pp. 251-266, 2001.

[8] A. C. Guyette, I. C. Hunter, and R. D. Pollard, "Exact synthesis of microwave filters with nonuniform dissipation," in *Microwave Symposium IEEE MTT-S International, Hawaii*, 2007, pp. 537-540.

[9] A. C. Guyette, "Optimum Design of Microwave Filters with Finite Dissipation," in *School of Electronic and Electrical Engineering*, vol. Doctor of Philosophy UK: The University of Leeds, July 2006.

[10] K. Wu, "Integration and interconnect techniques of planar and non-planar structures for microwave and millimeter-wave circuits - current status and future trend," in *Microwave Conference, 2001. APMC 2001. 2001 Asia-Pacific*, 2001, pp. 411-416 vol.2.

[11] C. Xiaoping, H. Wei, T. Cui, C. Jixin, and W. Ke, "Substrate integrated waveguide (SIW) linear phase filter,"

- Microwave and Wireless Components Letters, IEEE, vol. 15, pp. 787-789, 2005.
- [12] C. Xiaoping, H. Zhangchen, H. Wei, C. Tiejun, and W. Ke, "Planar asymmetric dual-mode filters based on substrate integrated waveguide (SIW)," in Microwave Symposium Digest, 2005 IEEE MTT-S International, 2005, p. 4 pp.
- [13] X. Chen, W. Hong, T. Cui, Z. Hao, and K. Wu, "Substrate integrated waveguide elliptic filter with transmission line inserted inverter," Electronics Letters, vol. 41, pp. 851-852, 2005.
- [14] D. Deslandes and K. Wu, "Design Consideration and Performance Analysis of Substrate Integrated Waveguide Components," in European Microwave Conference, 2002. 32<sup>nd</sup>, 2002, pp. 1-4.
- [15] D. Deslandes and W. Ke, "Single-substrate integration technique of planar circuits and waveguide filters," Microwave Theory and Techniques, IEEE Transactions on, vol. 51, pp. 593-596, 2003.
- [16] B. H. Ahmad, "Substrate Integrated Waveguide Bandstop Filters," in School of Electrical and Electronic Engineering, vol. Doctor of Philosophy UK: The University of Leeds, March 2008.
- [17] I. Hunter, Theory and Design of Microwave Filters. United Kingdom: The Institution Of Electrical Engineers, 2001.
- [18] B. B. Z. Sotoodeh, F. H. Kashani, H. Ameri, "A novel bandpass waveguide filter structure on SIW technology," Progress in Electromagnetics Research Letters, vol. 2, p. 8, 2008.
- [19] C. Xiao-Ping, H. Liang, and W. Ke, "Synthesis and Design of Substrate Integrated Waveguide Filter Using Predistortion Technique," in Microwave Conference, 2007. APMC 2007. Asia-Pacific, 2007, pp. 1-4.
- [20] J. C. Bohorquez, B. Potelon, C. Person, E. Rius, C. Quendo, G. Tanne, and E. Fourn, "Reconfigurable Planar SIW Cavity Resonator and Filter," in Microwave Symposium Digest, 2006. IEEE MTT-S International, 2006, pp. 947-950.
- [21] D. M. Pozar, Microwave Engineering. Hoboken, NJ: John Wiley & Sons, Inc., 2005.
- [22] B. Potelon, J. F. Favennec, C. Quendo, E. Rius, C. Person, and J. C. Bohorquez, "Design of a Substrate Integrated Waveguide (SIW) Filter Using a Novel Topology of Coupling," Microwave and Wireless Components Letters, IEEE, vol. 18, pp. 596-598, 2008.

